Published in final edited form as:
Liver Transpl. 2012 June ; 18(6): 727–736. doi:10.1002/lt.23413.

Imaging Predictors of Response to Transarterial Chemoembolization in Patients with Hepatocellular Carcinoma: Radiologic-Pathologic Correlation

Sharon W. Kwan, MD[1], **Nicholas Fidelman, MD**[2], **Elizabeth Ma, BS**[3], **Robert K. Kerlan Jr., MD**[2], and **Francis Y. Yao, MD**[3]

[1]Department of Radiology, University of Washington, Seattle, WA

[2]Department of Radiology and Biomedical Imaging, University of California, San Francisco, San Francisco, CA

[3]Department of Medicine, University of California, San Francisco, San Francisco, CA

Abstract

Transarterial chemoembolization (TACE) is one of the standard therapies for bridging patients with hepatocellular carcinoma (HCC) to transplantation. This study aimed to determine which features on pre- and post-TACE imaging are associated with tumor necrosis on pathologic specimens. Records of 105 patients with 132 HCC lesions who underwent liver transplantation following TACE were retrospectively reviewed. Greater than 90% necrosis was achieved in 70% of nodules. Development of greater than 90% lesion necrosis at pathology was associated with avid lesion enhancement (p=0.03) and presence of a feeding vessel larger than 0.9 mm in diameter on the pre-TACE visceral angiogram (p=0.008). Near-complete lesion necrosis was also associated with extensive ethiodized oil accumulation within a lesion during TACE administration (p=0.02). On post-TACE computed tomography, lack of residual contrast enhancement (p<0.0001), decrease in lesion size (p=0.009), high lesion density due to ethiodized oil accumulation (p=0.005), and diffuse distribution of ethiodized oil throughout the lesion (p<0.0001) were also correlated with near-complete lesion necrosis at pathology. In conclusion, this study found multiple pre-TACE and post-TACE imaging characteristics of HCC which were associated with near complete tumor necrosis at histopathology following TACE. These findings may help guide selection of an optimal treatment strategy for bridging patients with HCC to liver transplant.

Keywords

Locoregional therapy; Angiography; Computed Tomography

Hepatocellular carcinoma (HCC) is one of the most common malignancies worldwide (1) and its incidence is expected to continue to rise (2). Only a minority of patients with HCC

Address correspondence to: Nicholas Fidelman, MD, UCSF Department of Radiology, 505 Parnassus Avenue, Room M-361, San Francisco, CA 94143, Telephone: 415-353-1300, Fax: 415-353-8570, Nicholas.Fidelman@ucsf.edu.

qualify for surgical resection, and liver transplantation is the definitive therapy available for patients with unresectable HCC (3). Unfortunately, the limited supply of available donor organs results in prolonged wait times and patient dropout is a serious problem (4). In order to keep tumor growth under control during the waiting period, multiple bridging locoregional treatment strategies are used, of which transarterial chemoembolization (TACE) is one of the most widely employed. At certain centers, locoregional therapies have also been used to down-stage patients to meet transplant criteria (5). Despite its widespread use in patients awaiting transplantation, the evidence is not conclusive that TACE prior to transplantation leads to improved outcomes. Furthermore, these procedures are not without inherent risks and complications.

There is some evidence to support the goal of achieving complete tumor necrosis by locoregional therapy in the pre-transplant setting. Studies in patients with HCC undergoing liver transplantation have demonstrated that complete necrosis in explanted livers is predictive of very low recurrence rates (6, 7) and conversely, that incomplete necrosis is correlated with disease recurrence (8). Nonetheless, it is not known which, if any, pre-treatment imaging characteristics of HCC lesions are predictive of complete necrosis on histopathology following TACE. If certain characteristics are found to be associated with response, then patients with HCC exhibiting these characteristics would be more likely to benefit from TACE. In HCC without favorable characteristics, alternative or adjuvant treatments or even no treatment may be considered.

The experience with correlating imaging features of HCC lesions following TACE with findings at pathology has been limited (9-13), since only a minority of patients are candidates for resection or liver transplantation. Nevertheless, it has been suggested that dense tumor stain with ethiodized oil (12) and lack of residual enhancement (9, 11, 13) on post-TACE computed tomography (CT) are associated with greater extent of tumor necrosis at pathology. Since cross-sectional imaging remains an essential tool in diagnosing recurrent or residual disease following liver-directed therapy, identification of reliable imaging predictors of tumor response to TACE is important. Confident recognition of undertreated tumor regions and early detection of recurrence might subsequently lead to more effective eradication of untreated HCC.

In view of these considerations, the purpose of our study was to determine which angiographic and CT imaging characteristics of HCC tumors before and after TACE are associated with greater tumor response, as measured by the extent of necrosis on histopathologic examination on the explanted liver following liver transplantation.

Materials and Methods

Patient Population

This study was approved by the Institutional Review Board with waiver of informed consent. We identified all patients who underwent liver transplantation for HCC between January 2002 and January 2009 who had undergone TACE at least one week prior to transplantation. HCC was diagnosed by percutaneous biopsy or if imaging demonstrated a hypervascular lesion in the setting of liver cirrhosis and elevated serum alpha-fetoprotein

level. All of these patients were deemed to have HCC not suitable for surgical resection or ablative therapy on the basis of tumor size, lesion location, or underlying liver dysfunction. Lesions that were also treated with other locoregional therapies, such as radiofrequency ablation or percutaneous ethanol injection, were excluded.

The final patient population included 105 patients (85 men and 20 women, mean age 58 years, age range 38-77 years) with 132 HCC lesions. Retrospective review of medical records was conducted to identify the etiology of liver disease and to determine the Childs-Pugh score. The total number of TACE procedures performed on each lesion and the time interval between the first TACE and transplantation were obtained from the medical records. Lesion sizes and location were determined from the last cross-sectional imaging study prior to TACE.

The demographics of the final patient population and HCC lesion characteristics are shown in Table 1.

CT technique

CT examinations were performed using a 4- or 16-detector row scanner (LightSpeed LX/i; GE Medical Systems, Milwaukee, WI). The abdomen was imaged from the dome of the diaphragm to the iliac crests. Contrast used was 150 mL of iohexol (Omnipaque-350; GE Healthcare, Princeton, NJ), injected intravenously through a power injector at a rate of 4–5 mL/sec. Multiphase CECT included contiguous noncontrast images with a 5 mm collimation followed by late arterial images with 20 sec delay and 2.5 mm collimation and portal venous phase images with 70 sec delay and 2.5 mm collimation.

TACE technique

TACE was performed after patients provided written informed consent. A 5-French catheter was inserted into the common femoral artery and angiographic survey of the celiac and superior mesenteric arteries was performed. Digital subtraction angiography was also performed after selective catheterization of the proper, right and/or left hepatic arteries. All angiographic images were sent to a picture archiving and communication system. Vessels supplying one or two hepatic segments were selected with a coaxially placed microcatheter (Renegade HI-FLO, Boston Scientific, Natick, MA). Chemoembolization was performed with an emulsion of 25 mg doxorubicin hydrochloride, 10 mg mitomycin C, 50 mg cisplatin, and ethiodized oil (Ethiodol; Laboratoires Guerbet, Roissy, France). The administered doses of chemotherapy agents were adjusted in patients with liver or renal dysfunction, leukopenia, and thrombocytopenia. Administration of the emulsion was followed by embolization with a slurry of gelatin sponge (Gelfoam, Pharmacia-Upjohn, Kalamazoo, MI) until stasis was achieved.

Review of Imaging Findings

Two radiologists (Reader 1 N.F., and Reader 2 S.W.K. with 6 and 3 years' of experience with abdominal imaging and angiography, respectively) retrospectively reviewed the angiographic and CT studies performed prior to and following TACE on all patients. In all cases, angiographic evaluations were performed as part of the chemoembolization

procedure. The readers reviewed all images independently on a workstation and were blinded to patient and histopathological outcome.

For angiographic studies, each HCC lesion was assigned scores by each reader based on the degree of enhancement (0=mild-moderate, 1=avid) and diameter of the largest feeding artery (0=smaller than the diameter of a microcatheter, 1=equal or larger than the diameter of a microcatheter), and ethiodized oil deposition within the target lesion (evaluation based on a digital fluoroscopic image obtained prior to removal of the angiographic catheter; 0=minimal-moderate, 1=extensive). For pre-TACE CT studies, each HCC lesion was assigned scores by each reader based on the degree of enhancement (0=mild-moderate, 1=avid) and degree of contrast washout on portal-venous imaging phase (0=none-moderate, 1=extensive).

Locations of the HCC lesions were classified as “favorable” or “unfavorable” based on the authors' experience with selective catheterization of segmental hepatic artery branches supplying a tumor. Lesion location was classified as unfavorable if the lesion was centered in Couinaud segments 1 or 4, or if the lesion border was within 1 cm of the liver dome. Location in segments 1 and 4 were considered unfavorable because tumors in these segments are frequently supplied by small-diameter feeding arteries and therefore selective catheterization and administration of adequate amounts of embolic material often challenging. Lesions located near the liver dome are sometimes difficult to identify angiographically due to respiratory motion. All other lesions were classified as favorable in location.

Mean lesion density on CT in Hounsfield units (HU) was measured by a single radiologist (N.F.) in a manner described as follows. A circular region of interest (ROI) for each lesion was drawn to encompass the longest dimension of the enhancing portion of each lesion on arterial phase imaging, using the transaxial image corresponding to the center of the Z-axis of each lesion. This measurement was recorded as $HU_{arterial}$. The reader subsequently drew the same ROI on the corresponding venous and noncontrast phase images with measurements corresponding to HU_{venous} and $HU_{noncontrast}$, respectively. Two objective characteristics were calculated for each lesion: measured enhancement ($HU_{arterial}$− $HU_{noncontrast}$) and measured washout ($HU_{arterial}$− HU_{venous}).

Following TACE, CT studies were independently evaluated by the readers with respect to residual lesion enhancement (0=absent; 1=present), ethiodized oil distribution within a lesion (0=none, patchy, or partial lesion coverage; 1=diffuse), ethiodized oil density within a lesion (0=none-moderate, 1=high). Ethiodized oil accumulation was also estimated quantitatively by calculating the difference between HU from an ROI drawn over the lesion on the pre-contrast phase of a CT scan ($HU_{lipiodol}$) and HU from an ROI drawn over the background liver ($HU_{background}$). Other quantitative measurements included single longest lesion dimension and enhancing component ratio. Enhancing component ratio was calculated as the difference of single longest enhancing dimension and single longest dimension of ethiodized oil deposition area divided by the single longest enhancing dimension.

Correlation with Histopathology

All explanted livers were processed according to routine clinical protocol, with the freshly explanted livers sliced serially at 10 mm intervals. Macroscopically visible neoplastic nodules were evaluated with microscopy after hematoxylin and eosin staining. Since 2001, reporting of explant tumor pathology in all patients who underwent liver transplant for HCC was standardized as follows: Percentage necrosis was defined as the volume of necrotic areas divided by the total tumor volume and was classified into one of the following ranges: <30%, 30-60%, 61-90%, 91-99%, and 100%. In the present study, we focused on patients with > 90% tumor necrosis and radiologic and angiographic factors associated with > 90% necrosis from TACE.

We retrospectively reviewed pathology reports to extract data on tumor size, tumor location, tumor grade, and percentage of necrosis for all lesions. Two weeks after assigning imaging finding scores and remaining blinded to those scores, two readers (N.F. and S.W.K.) correlated by consensus the location of lesions described on gross pathology with the location of lesions on imaging, using all available imaging studies. No corresponding HCC lesion was seen on histopathology for 12 of the treated lesions. In addition, the location of five lesions within the explanted organs could not be correlated to the CT images by consensus, and six lesions were identified as HCC on pathology, but no percentage necrosis was reported. These 23 lesions were excluded from the statistical analysis.

Statistical Analysis

Characteristics of the study population were summarized with means and ranges for continuous measures. Tabulations and percentages were used to summarize categorical variables.

Using logistical regression with generalized estimating equation models, we modeled the odds of “near complete necrosis” (defined as >90% necrosis) in the explanted organs. Generalized estimating equation models are a general method for incorporating within-subject correlation in a generalized linear model (14) that accounts for the statistical dependence among multiple lesions in the same individual. The histopathology classification of necrosis (near complete versus incomplete) was the dependent outcome variable for all models. Independent patient and lesion characteristics were included as covariates in the final multivariate models only if univariate analysis demonstrated association with the outcome variable at the $p < 0.20$ level. We chose this p-value cut-off to be more conservative in our adjusted multivariate models. Based on this criterion, the final multivariate models for pre-TACE imaging findings adjusted for patients' Child-Pugh class, time from first TACE to transplant for each lesion, and total number of TACE procedures performed on each lesion. The final multivariate model for post-TACE imaging findings adjusted for patients' Child-Pugh class, time from first TACE to transplant for each lesion, and gender. Independent variables were considered significantly associated with the outcome if the 95% confidence interval for the odds ratio excluded one. Kappa statistic was calculated to measure inter-reader agreement. All analyses were conducted in SAS Version 9.2 (SAS Institute, Cary, NC).

Results

Characteristics of the patients and HCC lesions included in this study are summarized in Table 1. Complete pre-TACE angiography and CT imaging data were available for 87 patients with 109 HCC lesions. Complete data on follow-up imaging with contrast-enhanced multiphase CT performed following TACE and prior to liver transplantation was available for 79 patients with 102 HCC lesions. The number of HCC lesions per patient ranged from one to three.

The majority of lesions were successfully treated with TACE. On histopathology 62 (57%) lesions were 100% necrotic, and 14 (13%) lesions were 91-99% necrotic. These tumors together comprised the “near complete necrosis” outcome group and represented 70% of all lesions. Conversely, 6 (6%) lesions were 61-90% necrotic, 10 (9%) were 30-60% necrotic, and 17 (16%) were <30% necrotic on histopathology.

Odds ratios (ORs) for the outcome by pre-TACE patient and lesion characteristics are summarized in Table 2. Of all the characteristics considered, Child-Pugh classification was the most highly associated with near complete necrosis at histopathology. Patients with Child-Pugh class B or C cirrhosis had lower odds of near complete necrosis compared patients with Child-Pugh class A liver disease, with the odds worsening with progressively higher severity of liver disease (Class B OR 0.20 [0.07-0.61]; Class C OR 0.14 [0.04-0.47]). Increasing time interval between first TACE and transplantation was also significantly associated with higher odds of near complete necrosis (OR per 30 days 1.20 [1.06-1.36]). No other patient or lesion characteristics were significantly associated with near complete necrosis at the $p<0.05$ level.

Of all the imaging findings performed prior to TACE, only angiographic imaging findings were found to be significantly associated with development of near complete necrosis following TACE (Table 3). The angiographic finding of avid lesion enhancement (Figure 1A) was highly associated with increased odds of near complete necrosis by histopathology for both readers (Reader 1 OR 3.49 [1.12-10.87]; Reader 2 OR 4.46 [1.52-13.11]). This finding was noted for 81% of lesions displaying >90% necrosis at pathology according to reader 1 (83% of lesions according to reader 2). The angiographic finding of a feeding vessel with a diameter larger than that of a microcatheter (0.9 mm) was also associated with increased odds of near complete necrosis for one reader (Reader 1 OR 5.04 [1.44-17.60]). For the other reader, this association was borderline significant (Reader 2 OR 3.04 [0.99-9.37]). This finding was present for 79% of lesions that developed near-complete necrosis at pathology according to reader 1 (70% of lesions according to reader 2). Subjective appearance of an extensive amount of ethiodized oil deposited within the target lesion at the completion of TACE (Figure 1B) was also highly associated with the finding of >90% necrosis (Reader 1 OR 3.2 [1.08-9.5]; Reader 2 OR 2.9 [1.06-8.1]). According to reader 1, 81% of lesions (80% of lesions according to reader 2) with near-complete necrosis displayed this imaging feature. None of the CT findings prior to TACE were significantly associated with the histopathologic outcome.

Several imaging findings on post-TACE CT demonstrated a statistically significant correlation with development of >90% necrosis at histopathology (Table 4). Near complete necrosis on liver explants was highly associated with subjective absence of residual contrast enhancement on pre-transplant CT (Figure 2; Reader 1 OR 21.0 [5.2-87]; Reader 2 OR 15.7 [3.2-77]) and with lower calculated enhancing component ratios (OR 0.09 [0.02-0.41]). Subjective findings of diffuse ethiodized oil distribution throughout the lesion (Reader 1 OR 15.5 [3.9-62]; Reader 2 OR 16.9 [4.2-67]) and high ethiodized oil accumulation within a lesion (Reader 1 OR 16.9 [1.3-78]; Reader 2 OR 15.2 [1.2-95]), as well as higher quantitative ethiodized oil accumulation (Density per 100 HU OR 1.21 [1.06-1.38]) were also associated with >90% necrosis. A similar association was also found for progressive decrease in lesion size (OR 37 [2.1-647]). Partial or patchy distribution of ethiodized oil throughout the treated lesion (Figure 3) was associated with less extensive necrosis at pathology.

There was good to very good agreement between the two readers for all subjectively scored imaging features, with kappa values ranging from 0.71-0.91.

Discussion

TACE is the mainstay palliative liver-directed treatment modality for HCC, which has been proven to confer survival benefit compared to supportive care primarily in patients with good functional reserve (15, 16). This treatment modality is also frequently being used as a bridge to transplantation. However, efficacy of TACE for this indication is not yet proven. One reason for the lack of evidence of improved survival post-transplant may be due to variable tumor response to TACE. If tumors that are most likely to respond to TACE can be selected based on specific imaging characteristics, overall outcomes may improve. Those lesions with imaging characteristics predictive of incomplete response may benefit from alternative or adjuvant forms of therapy.

The existing literature reports rates of complete histopathologic tumor response to TACE of 26-83% (17-21). This wide range is largely related to heterogeneity in patient population, TACE technique, and definitions of complete response. Our study found a rate of near complete histopathologic necrosis of 70%. This number may be towards the higher end of the reported range for two main reasons. First, our study group included only those patients who were successfully bridged or downstaged to transplantation, and thus included tumors with indolent biology or more responsive to treatment. Secondly, all of our study patients underwent TACE targeting one or two liver segments. Such selective TACE has been found to result in higher rates of histopathologic necrosis compared to lobar or nonselective TACE (17).

We found that two non-imaging related variables were highly correlated to near complete histopathologic response to TACE: 1) lower Child-Pugh score and 2) longer time between first TACE procedure and transplant. The first finding likely contributes to the improved outcomes seen in patients with lower Child-Pugh scores compared to those with more severe disease, a consistent finding in the literature (22-24). This may be in part related to the less aggressive treatment regimen (with reduced doses of chemotherapy agents) that patients

with more severe liver disease received. With respect to the second finding, the longer time between TACE and transplant may reflect the fact that lesions found to have near complete necrosis after TACE are less prone to local or systemic recurrence, thus allowing patients to remain on a waiting list until an organ becomes available.

After controlling for non-imaging related variables, we found that several angiographic imaging findings were associated with near complete necrosis on histopathology. For both readers, the odds of near complete necrosis for a tumor demonstrating avid enhancement were about 3-4 times higher than for a tumor that showed only mild to moderate enhancement. Additionally, the odds of near complete necrosis for a tumor demonstrating a feeding artery with a diameter equal to or wider than 0.9 mm was about 3-5 times higher than for a tumor which was fed by an artery smaller than that size threshold, although the results was only nearing statistical significance for the less experienced reader. These findings suggest that the degree and type of vascular flow to a tumor affects its response to TACE. While the precise mechanism for this is subject for future studies, we offer a few possible explanations. HCC tumors derive varying ratios of blood flow from the hepatic arteries versus portal veins, and those with more preserved portal blood flow are expected to have less well developed feeding arteries and have been shown to enhance less on CT hepatic arteriography (25, 26). It is possible that these are tumors that maintain enough portal blood flow such that agents delivered transarterially would access less of the tumor and therefore be less effective. Similarly, when the feeding arteries are embolized, these tumors could maintain enough portal blood flow to avoid hypoxia. Altered tissue architecture of these tumors may also provide a mechanism for our findings. Vascular endothelial growth factor and other angiogenic factors are upregulated to varying degrees in HCC. The former has been demonstrated to result in disruption of tight junctions (27), resulting in increased endothelial permeability. Thus, those tumors with high vascular endothelial growth factor expression and therefore greater neovascularity may also be more susceptible to transarterial therapy as the more “leaky” tissues allow for better penetration of antineoplastic agents.

Increased tumor vascularity may have also resulted in more avid accumulation of ethiodized oil on post-TACE fluoroscopic and CT images within the more necrotic lesions. This finding was also observed by Takayasu et al. (9) and Choi et al. (12) who demonstrated that tumor portions that retained ethiodized oil were more likely to be necrotic at pathology. Similarly, Riaz et al. (13) found that 82% of lesions demonstrating complete necrosis at post-TACE MRI were completely necrotic at pathology. Conversely, lesions demonstrating incomplete staining with ethiodized oil and residual enhancement were more likely to contain extensive regions of viable tumor. This finding corroborates the work of Takayasu et al. (10), Herber et al. (11), and Riaz et al. (13).

It is notable that none of the imaging findings on pre-TACE CT was significantly correlated with histopathologic outcomes. A likely explanation for this is that our CT imaging technique had an insufficient level of precision to differentiate between tumors to the same extent that we saw with angiography. Because we used CT studies obtained under our routine clinical protocol, the density of intravenous contrast bolus was subject to typical variations seen in clinical practice, including intravenous catheter size and location, patients'

cardiovascular physiology, and exact timing of each acquisition. All of these factors result in wider variation in the contrast enhancement pattern in the tumors as compared to a selective intra-arterial contrast injection with dynamic angiographic imaging. CT imaging techniques that are specifically designed to assess vascularity, such as CT perfusion, may prove to be another tool to predict HCC tumor response to TACE. However, these techniques are still in the early stages of development and, for this study, we wanted to focus on imaging studies acquired as part of routine clinical practice.

There are several limitations of the present study. The main limitation is its retrospective design. The aspect that was particularly prone to uncertainty from the use of retrospective data was the correlation of imaging findings to histopathology. Furthermore, the explanted specimens were reviewed by clinical pathologists as part of routine clinical practice and the degree of necrosis was determined in a subjective manner. However, these pathologists adhered to reporting standards that were developed at our institution specifically for evaluation of liver explants. Our analysis was focused on near complete or complete tumor necrosis (> 90% necrosis), but we cannot exclude microscopic foci of viable tumors with slicing of the livers at 10 mm. We designed this study to examine the relationship of imaging characteristics with pathological outcome, but the observational nature of this study cannot exclude confounders which may have affected outcomes. Since only patients who were successfully bridged to liver transplant were included in the evaluation of radiologic-pathologic correlation, our findings may reflect a selected subgroup whose tumors were less aggressive and more responsive to TACE. None of our patients had hypovascular HCC, because decisions were made to treat these tumors with alternative therapies rather than TACE. This study was also not powered to determine if response to TACE correlates with reduced rate of tumor recurrence and improved survival post-transplant. Despite these limitations, our data represent one of the largest patient cohorts in the literature for whom imaging findings of HCC have been correlated with outcomes on histopathology. Furthermore, angiographic imaging features predictive of the degree of tumor necrosis following TACE have not been previously reported in the literature. As such, this study provides new information that may be useful in clinical practice to define the best treatment strategies for patients with HCC prior to liver transplantation.

In summary, we found that several pre-TACE angiographic imaging findings of HCC, such as avid contrast enhancement and feeding artery size greater than 0.9 mm as well as multiple CT imaging features post-TACE, including absence of residual enhancement and extensive ethiodized oil accumulation, were associated with near complete tumor necrosis at histopathology following TACE. These findings may help guide selection of an optimal treatment strategy for bridging patients with HCC to liver transplant.

Acknowledgments

S.W.K. was supported by the National Institute of Biomedical Imaging and Bioengineering Grant NIH/NIBIB T32 EB001631-05.

Statistical consulting was supported by NIH/NCRR UCSF-CTSI Grant Number UL1 RR024131.

References

1. Parkin DM, Bray F, Ferlay J, Pisani P. Global cancer statistics, 2002. CA Cancer J Clin. 2005; 55:74–108. [PubMed: 15761078]
2. El-Serag HB, Davila JA, Petersen NJ, McGlynn KA. The continuing increase in the incidence of hepatocellular carcinoma in the United States: an update. Ann Intern Med. 2003; 139:817–823. [PubMed: 14623619]
3. Llovet JM, Schwartz M, Mazzaferro V. Resection and liver transplantation for hepatocellular carcinoma. Semin Liver Dis. 2005; 25:181–200. [PubMed: 15918147]
4. Yao FY, Bass NM, Nikolai B, Merriman R, Davern TJ, Kerlan R, et al. A follow-up analysis of the pattern and predictors of dropout from the waiting list for liver transplantation in patients with hepatocellular carcinoma: implications for the current organ allocation policy. Liver Transpl. 2003; 9:684–692. [PubMed: 12827553]
5. Yao FY, Kerlan RK, Hirose R, Davern TJ, Bass NM, Feng S, et al. Excellent outcome following down-staging of hepatocellular carcinoma prior to liver transplantation: an intention-to-treat analysis. Hepatology. 2008; 48:819–827. [PubMed: 18688876]
6. Sotiropoulos GC, Malago M, Molmenti EP, Malago M, Molmenti EP, Radtke A, et al. Disease course after liver transplantation for hepatocellular carcinoma in patients with complete tumor necrosis in liver explants after performance of bridging treatments. Eur J Med Res. 2005; 10:539–542. [PubMed: 16356871]
7. Majno PE, Adam R, Bismuth H, Castaing D, Ariche A, Krissat J, et al. Influence of preoperative transarterial lipiodol chemoembolization on resection and transplantation for hepatocellular carcinoma in patients with cirrhosis. Ann Surg. 1997; 226:688–701. discussion 701-703. [PubMed: 9409568]
8. Ravaioli M, Grazi GL, Ercolani G, Fiorentino M, Cescon M, Golfieri R, et al. Partial necrosis on hepatocellular carcinoma nodules facilitates tumor recurrence after liver transplantation. Transplantation. 2004; 78:1780–1786. [PubMed: 15614151]
9. Takayasu K, Arii S, Matsuo N, Yoshikawa M, Ryu M, Takasaki K, et al. Comparison of CT findings with resected specimens after chemoembolization with iodized oil for hepatocellular carcinoma. AJR Am J Roentenol. 2000; 175:699–704.
10. Takayasu K, Moriyama S, Muramatsu Y, Suzuki M, Yamada T, Kishi K, Hasagawa H, Okazaki N. Hepatic arterial embolization for hepatocellular carcinoma: Comparison of CT scans and resected specimens. Radiology. 1984; 150:661–665. [PubMed: 6320253]
11. Herber S, Biesterfeld S, Franz U, Schneider J, Thies J, Schuchmann M, Duber C, et al. Correlation of multislice CT and histomorphology in HCC following TACE: Predictors of outcome. Cardiovasc Intervent Radiol. 2008; 31:768–777. [PubMed: 18196335]
12. Choi BI, Kim HC, Han JK, Park JH, Kim YI, Kim ST, et al. Therapeutic effect of transcatheter oily chemoembolization therapy for encapsulated nodular hepatocellular carcinoma: CT and pathologic findings. Radiology. 1992; 182:709–713. [PubMed: 1311116]
13. Riaz A, Lewandowski RJ, Kulik L, Ryu RK, Mulcahy MF, Baker T, et al. Radiologic–Pathologic Correlation of Hepatocellular Carcinoma Treated with Chemoembolization. Cardiovasc Intervent Radiol. 2010; 33:1143–1152. [PubMed: 19967371]
14. Zeger SL, Liang KY. Longitudinal data analysis for discrete and continuous outcomes. Biometrics. 1986; 42:121–130. [PubMed: 3719049]
15. Llovet JM, Real MI, Montana X, Planas R, Coll S, Aponte J, et al. Arterial embolisation or chemoembolisation versus symptomatic treatment in patients with unresectable hepatocellular carcinoma: a randomised controlled trial. Lancet. 2002; 359:1734–1739. [PubMed: 12049862]
16. Lo CM, Ngan H, Tso WK, Liu CL, Lam CM, Poon RT, et al. Randomized controlled trial of transarterial lipiodol chemoembolization for unresectable hepatocellular carcinoma. Hepatology. 2002; 35:1164–1171. [PubMed: 11981766]
17. Golfieri R, Cappelli A, Cucchetti A, Piscaglia F, Carpenzano M, Peri E, et al. Efficacy of selective transarterial chemoembolization in obtaining tumor necrosis in small (<5 cm) hepatocellular carcinomas. Hepatology. 2011; 53:1580–9. [PubMed: 21351114]

18. Takayasu K, Shima Y, Muramatsu Y, Moriyama N, Yamada T, Makuuchi M, et al. Hepatocellular carcinoma: treatment with intraarterial iodized oil with and without chemotherapeutic agents. Radiology. 1987; 163:345–351. [PubMed: 3031724]
19. Bismuth H, Morino M, Sherlock D, Castaing D, Miglietta C, Cauquil P, Roche A. Primary treatment of hepatocellular carcinoma by arterial chemoembolization. Am J Surg. 1992; 163:387–394. [PubMed: 1373044]
20. Higuchi T, Kikuchi M, Okazaki M. Hepatocellular carcinoma after transcatheter hepatic arterial embolization. A histopathologic study of 84 resected cases. Cancer. 1994; 73:2259–2267. [PubMed: 7513245]
21. Graziadei IW, Sandmueller H, Waldenberger P, Koenigsrainer A, Nachbaur K, Jaschke W, et al. Chemoembolization followed by liver transplantation for hepatocellular carcinoma impedes tumor progression while on the waiting list and leads to excellent outcome. Liver Transpl. 2003; 9:557–563. [PubMed: 12783395]
22. Kim JH, Kim JH, Choi JH, Kim CH, Jung YK, Yim HJ, et al. Value of the model for end-stage liver disease for predicting survival in hepatocellular carcinoma patients treated with transarterial chemoembolization. Scand J Gastroenterol. 2009; 44:346–357. [PubMed: 18991165]
23. Brown DB, Fundakowski CE, Lisker-Melman M, Crippin JS, Pilgram TK, Chapman W, Darcy MD. Comparison of MELD and Child-Pugh scores to predict survival after chemoembolization for hepatocellular carcinoma. J Vasc Interv Radiol. 2004; 15:1209–1218. [PubMed: 15525739]
24. Grieco A, Marcoccia S, Miele L, Marmiroli L, Caminiti G, Ragazzoni E, et al. Transarterial chemoembolization (TACE) for unresectable hepatocellular carcinoma in cirrhotics: functional hepatic reserve and survival. Hepatogastroenterology. 2003; 50:207–212. [PubMed: 12630024]
25. Tajima T, Honda H, Taguchi K, Asayama Y, Kuroiwa T, Yoshimitsu K, et al. Sequential hemodynamic change in hepatocellular carcinoma and dysplastic nodules: CT angiography and pathologic correlation. AJR Am J Roentgenol. 2002; 178:885–897. [PubMed: 11906868]
26. Asayama Y, Yoshimitsu K, Nishihara Y, Irie H, Aishima S, Taketomi A, Honda H. Arterial blood supply of hepatocellular carcinoma and histologic grading: radiologic-pathologic correlation. AJR Am J Roentgenol. 2008; 190:W28–34. [PubMed: 18094269]
27. Schmitt M, Horbach A, Kubitz R, Frilling A, Häussinger D. Disruption of hepatocellular tight junctions by vascular endothelial growth factor (VEGF): a novel mechanism for tumor invasion. J Hepatol. 2004; 41:274–283. [PubMed: 15288477]

Abbreviations

HCC	hepatocellular carcinoma
TACE	transarterial chemoembolization
HU	Hounsfield units
ROI	region of interest
OR	odds ratio

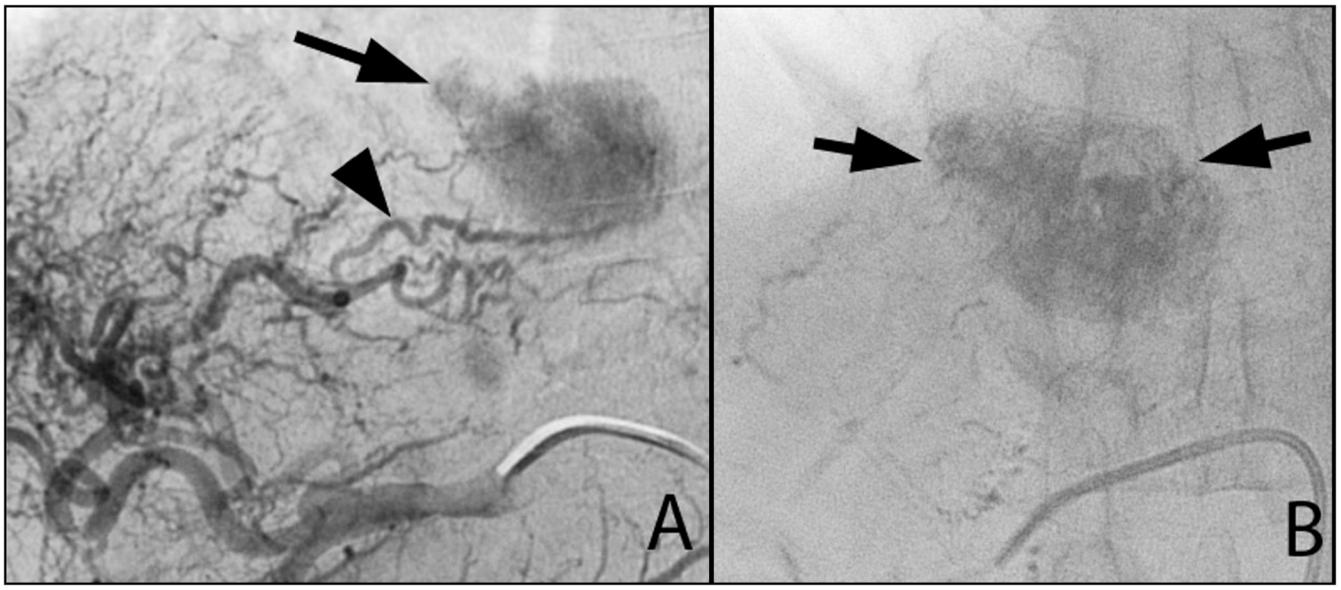

Figure 1.

Digital subtraction angiogram via a 5-French catheter demonstrates a hypervascular mass in the left liver lobe (A, arrows) supplied by a hepatic artery branch (A, arrowhead), the diameter of which is similar to that of the 5-French catheter (1.7 mm). Following TACE, extensive retention of radiodense ethiodized oil is present throughout the lesion (B, arrows).

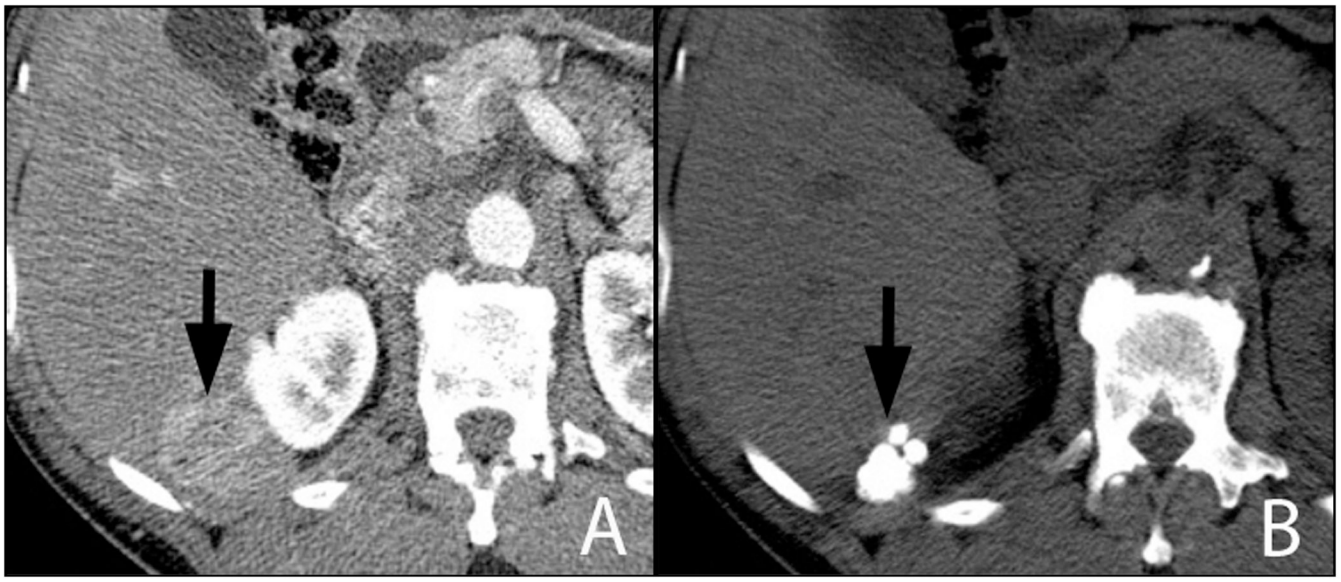

Figure 2.

Contrast-enhanced CT of the liver during arterial phase of imaging shows a hypervascular mass (A, arrow) adjacent to the right kidney. Repeat CT performed 3 months following TACE demonstrates extensive uptake of ethiodized oil and no residual enhancement within the lesion (B, arrow). This lesion was found to be 100% necrotic at pathology.

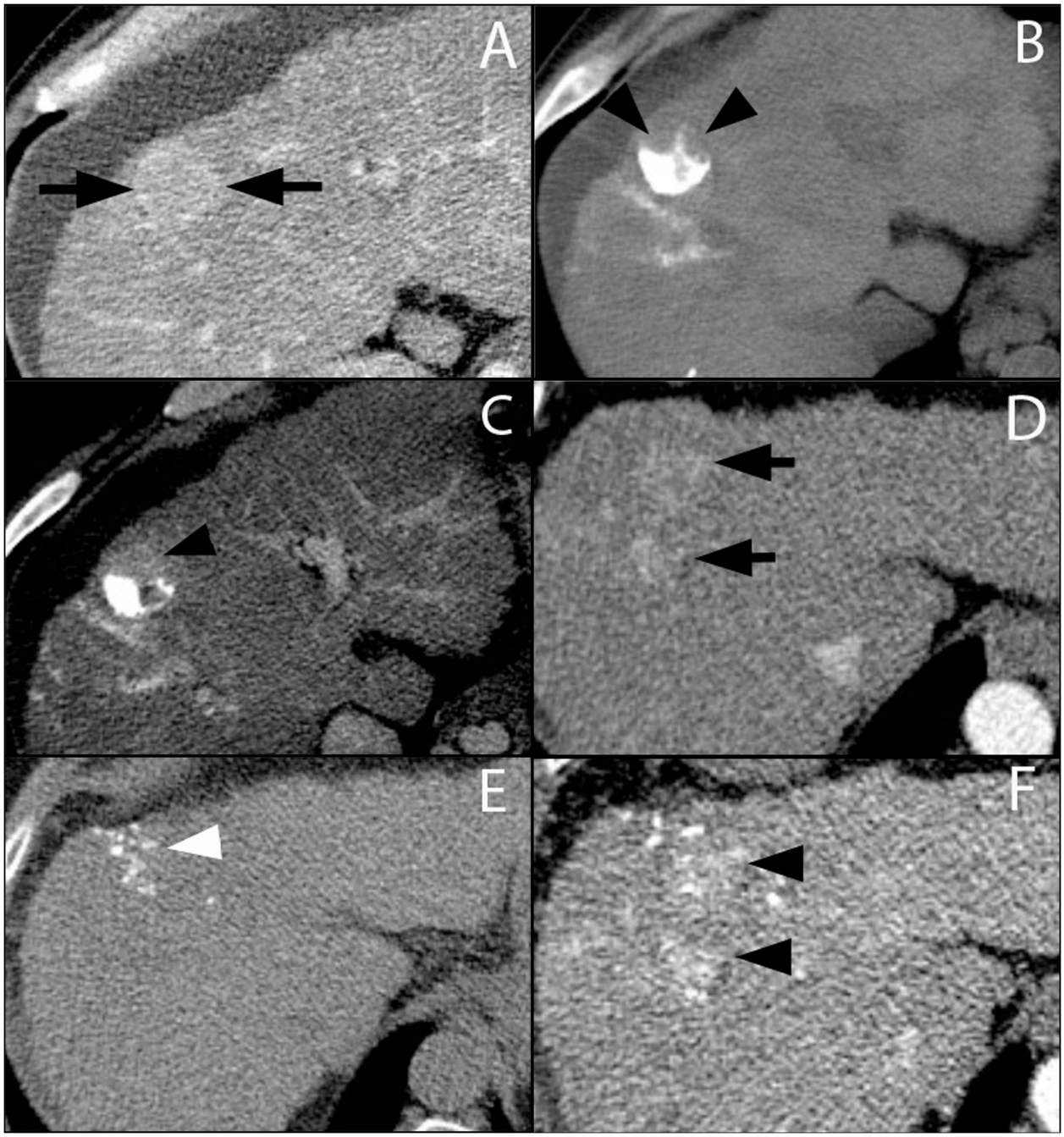

Figure 3.

Contrast-enhanced CT during the arterial phase demonstrates an enhancing lesion (A, arrows). Three months following TACE only the posterior aspect of the liver contains ethiodized oil (B, arrowheads). The anterior aspect of the lesion demonstrates residual enhancement (C, arrowhead), consistent with presence of residual viable tumor. Another contrast-enhanced CT example demonstrates a subtle hypervascular lesion (D, arrows). Minimal uptake of ethiodized oil was achieved within the lesion 3 months following TACE on the pre-contrast scan (E, arrowhead). Arterial phase of the post-contrast imaging

demonstrates extensive residual contrast enhancement within the lesion (F, arrowheads) consistent in appearance viable tumor regions.

Table 1

Patient Demographics.

Category	N (%)
Age (years)	
Mean	58
Range	38-77
Gender	
Female	20 (19)
Male	85 (81)
Etiology of liver disease	
Hepatitis B	24 (23)
Hepatitis C	64 (61)
Others	17 (16)
Child-Pugh class	
A	39 (37)
B	31 (30)
C	23 (22)
Unknown	12 (11)
Time from first TACE to transplant (days)	
Mean	197
Range	19-855
Lesions per patient	
Mean	1.3
Range	1-3
Size of lesion (cm)	
Mean	2.9
Range	0.8-7.5
Location of lesion	
Favorable for TACE *	110 (83)
Unfavorable for TACE *	22 (17)

* Please refer to Materials and Methods for the description of “favorable” and “unfavorable” lesion location for TACE

Table 2

Association of demographic, liver disease-specific, and lesion-specific variables with development of near complete tumor necrosis at histopathology.

Characteristic	Odds ratio	95% Confidence interval	P-value
Patient gender			
Female	1.0		
Male	1.7	0.7-4.2	0.29
Patient age			
per year	1.3	0.8-2.2	0.29
Patient Child-Pugh class			
A	1.0		
B	0.2	0.1-0.6	0.004
C	0.1	0.04-0.5	0.001
Etiology of liver disease			
HBV	1.0		
HCV	0.8	0.3-2.1	0.59
Multifactorial/other	0.5	0.2-1.9	0.34
Time between first TACE and transplant, by lesion			
per 30 days	1.2	1.1-1.4	0.005
Total number of TACE performed, by lesion			
1	1.0		
>1	0.4	0.2-1.2	0.10
Pre-TACE lesion size			
per cm	1.2	0.9-1.1	0.34
Lesion location			
Unfavorable for TACE	1.0		
Favorable for TACE	1.7	0.7-4.1	0.24

Table 3

Association of angiographic and CT imaging findings prior to and during TACE with development of near complete necrosis at histopathology.

Imaging finding	$N_{necrotic}/N_{observed}$ (%)	Odds Ratio [95% Confidence Interval]	P-value	Kappa
Subjective enhancement on angiography				
Reader 1				
Mild-moderate	34/55 (62)	1.0		
Avid	30/37 (81)	3.5 [1.1 - 10.9]	0.03	
Reader 2				0.71
Mild-moderate	31/52 (60)	1.0		
Avid	33/40 (83)	4.5 [1.5 - 13.1]	0.007	
Subjective artery diameter on angiography				
Reader 1				
Smaller than a microcatheter	45/68 (66)	1.0		
Greater or equal to microcatheter	19/24 (79)	5.0 [1.4 - 17.6]	0.01	
Reader 2				0.76
Smaller than a microcatheter	45/65 (69)	1.0		
Greater or equal to microcatheter	19/27 (70)	3.0 [0.99 - 9.0]	0.05	
Ethiodized oil accumulation within target lesion				
Reader 1				
Mild-moderate	32/52 (62)	1.0		
Extensive	21/26 (81)	3.2 [1.1 - 9.5]	0.04	
Reader 2				0.89
Mild-moderate	29/48 (60)	1.0		
Extensive	24/30 (80)	2.9 [1.1 - 8.1]	0.04	
Subjective enhancement on CT				
Reader 1				
Mild-moderate	51/72 (71)	1.0		
Avid	15/21 (71)	0.6 [0.2 - 2.1]	0.41	
Reader 2				0.79
Mild-moderate	50/71 (70)	1.0		
Avid	16/22 (73)	0.8 [0.2 - 2.8]	0.73	
Subjective washout on CT				
Reader 1				
None-moderate	54/81 (67)	1.0		
Extensive	11/21 (92)	3.1 [0.5 - 18.5]	0.22	
Reader 2				0.77
None-moderate	54/80 (68)	1.0		
Extensive	11/13 (83)	4.1 [0.7 - 25.1]	0.13	

Imaging finding	$N_{necrotic}/N_{observed}$ (%)	Odds Ratio [95% Confidence Interval]	P-value	Kappa
Measured enhancement on CT				
Per 10 HU	-	1.03 [0.9 - 1.2]	0.79	-
Measured washout on CT				
Per 10 HU	-	1.06 [0.9 - 1.2]	0.65	-

Table 4

Association of CT imaging findings following TACE with development of near complete necrosis at hstopathology.

Imaging finding	$N_{necrotic}/N_{observed}$ (%)	Odds Ratio [95% Confidence Interval]	P-value	Kappa
Subjective residual enhancement				
Reader 1				
Present	8/28 (29)	1.0		
Absent	49/56 (88)	21.0 [5.2 – 87]	<0.0001	
Reader 2				0.78
Present	5/21 (24)	1.0		
Absent	52/63 (83)	15.7 [3.2 - 77]	0.0007	
Enhancing component ratio	-	0.1 [0.02-0.41]	0.002	-
Subjective ethiodized oil distribution within lesion				
Reader 1				
None/Patchy/Partial	12/31 (39)	1.0		
Diffuse	45/53 (85)	15.5 [3.9 – 62]	0.0001	
Reader 2				0.91
None/Patchy/Partial	12/32 (38)	1.0		
Diffuse	45/52 (87)	16.9 [4.2 - 67]	0.002	
Subjective ethiodized oil accumulation within lesion				
Reader 1				
None/Mild/Moderate	12/28 (43)	1.0		
High	45/56 (80)	16.9 [1.3 - 78]	0.03	
Reader 2				0.91
None/Mild/Moderate	14/31 (45)	1.0		
High	43/53 (81)	15.2 [1.2 - 95]	0.04	
Measured accumulated ethiodized oil density				
Per 100 HU	-	1.2 [1.1 - 1.4]	0.005	-
Decrease in lesion size	55/82 (67)	37 [2.1 - 647]	0.01	-